Journal of Applied Polymer Science

The effects of surface-modified graphene nanoplatelets on the sliding wear properties of basalt fibers-reinforced epoxy composites

Elaheh Kazemi-Khasragh,[1] Farid Bahari-Sambran,[1] Seyed Mohammad Hossein Siadati,[1] Reza Eslami-Farsani,[1] Shabnam Arbab Chirani[2]

[1]K. N. Toosi University of Technology, Faculty of Materials Science and Engineering, No. 7, Pardis St., Mollasadra Avenue, Vanak Sq., Tehran, Iran

[2]ENI Brest, FRE CNRS 3744, IRDL, Brest, France

Correspondence to: F. Bahari-Sambran (E-mail: farid.bahari.1992@gmail.com)

ABSTRACT: Possessing unique designs and properties absent in conventional materials, nanocomposites have made a remarkable imprint in science and technology. This is particularly true regarding the polymer matrix composites when they are further reinforced with nanoparticles. In this study, the effects of different weight percentages (0, 0.1, 0.2, 0.3, 0.4, and 0.5) of surface-modified graphene nanoplatelets (GNPs) on the microhardness and wear properties of basalt fibers/epoxy composites were investigated. The GNPs were surface modified by silane, and the composites were made by the hand lay-up method. The wear tests were conducted under two different loads of 20 and 40 N. The best wear properties were achieved at 0.3 wt % GNPs as a result of the GNPs' self-lubrication property and the formation of a stable transfer/lubricating film at the pin and disk interface. Moreover, the friction coefficient was lower at the higher normal load of 40 N. The microscopic studies by FESEM and SEM showed that the presence of GNPs up to 0.3 wt % led to the stability of the transfer/lubricating film by enhancing the adhesion of the basalt fibers to the epoxy resin. © 2019 Wiley Periodicals, Inc. J. Appl. Polym. Sci. **2019**, *136*, 47986.

KEYWORDS: basalt fibers; graphene nanoplatelets; polymer matrix nanocomposites; wear properties

Received 2 January 2019; accepted 6 April 2019

DOI: 10.1002/app.47986

INTRODUCTION

Polymer matrix composites are one of the important types of engineering materials in various industries for their enhanced mechanical and abrasion properties.[1,2] Their fabrication can be tailored to make them suitable for various applications involving stress, wear, and high temperatures.[3] The tribology of polymer composites has progressively become important because of their growing applications in self-lubricating and sliding components as surface finishing materials such as seals, wheels, cams, rollers, clutches, and gears.[4,5]

One of the most widely used resins in fabricating polymer composites is the epoxy with high strength and modulus, low contraction, excellent heat resistance, and high chemical and corrosive resistance.[6] Although the epoxy matrix composites have excellent mechanical properties,[7] their wear properties are poor.[8] The use of reinforcing fibers improves their wear properties.[2,9] Basalt fibers, known as the green material of the 21st century, are non-toxic and non-combustible[10,11] and possess high wear resistance and hardness.[12] The incorporation of basalt fibers in the epoxy matrix has proven to improve the mechanical, thermal, and chemical properties of the resulting composites.[10,13]

The addition of nanoparticles such as graphene in the epoxy matrix has also been shown to improve the mechanical and wear properties of the resulting composites.[1,2,6,7] Graphene is a two-dimensional carbon material composed of sheets of sp^2-bonded carbon atoms, and it belongs to the family of carbon allotropes.[8,14] Graphene is the thinnest and strongest substance known in the world; it also has a high specific surface area (2630 m^2/g).[15] In graphene sheets, carbon atoms are linked in a hexagonal network. The structure of this material is perfect; hence, graphene has such good physical properties as electrical and thermal conductivity, high mechanical strength, transparency of about 98%, high flexibility, and thermal and mechanical resistance.[16,17] All of these properties have made graphene a great filler in composites.[15,18] In addition, for wear applications, the easy sliding of graphene nanoplatelets (GNPs) reduces the adhesion and friction of contacting surfaces.[19]

The uniform dispersion of nanoparticles in the matrix is one of the challenges encountered when fabricating nanocomposites. The difference in the surface energy between the nanoparticles and polymer materials leads to the agglomeration of nanoparticles in the matrix.[20] The weak dispersion of GNPs in the polymeric matrix weakens the mechanical properties of the composite.[18] To overcome this problem, GNPs are functionalized with organic molecules.[21,22] For this

© 2019 Wiley Periodicals, Inc.

purpose, many researchers have investigated the effect of surface modification of graphene and graphene oxide on the mechanical properties of composites.

Pan *et al.*,[18] for instance, investigated the tribological and mechanical properties of surface-modified graphene oxide-reinforced nylon. The results showed that the addition of graphene oxide greatly reduced wear and friction under dry sliding. The graphene-reinforced nanocomposite had lower wear rate when compared to the composite without graphene. Fang *et al.*[23] also addressed the surface structure and the tribological behavior of the epoxy resins coating reinforced with graphene and graphene oxide. Graphene and graphene oxide were added to the epoxy resin through chemical and physical modification, respectively. In this case, the ultrasound technology was used to improve the distribution and, consequently, the tribological behavior. The study of wear behavior showed that by the addition of graphene and graphene oxide, the friction coefficient decreased, and the wear properties improved. The coating containing 0.5 wt % graphene and 0.75 wt % graphene oxide had the lowest friction coefficient and the best wear resistance. Furthermore, Liu *et al.*[15] functionalized the GNPs using Diazonium, observing that at 0.3 wt %, the impact resistance of the nanocomposite improved by 39% at high temperature. Ren *et al.*[24] also studied the effect of adding different weight percentages of polythene-functionalized graphene on the wear behavior of the Nomex fabric/phenolic composite. Pin-on-disk tests were conducted in the force range of 94–251 N and sliding speeds of 0.28–0.73 m/s. They reported that the presence of 0.2 wt % functionalized graphene improved the wear properties.

When dealing with nanocomposites for tribological applications, other influential parameters include hardness, aspect ratio, particle size, orientation, concentration, and the reinforcement/matrix interface.[25] Furthermore, using two or more reinforcements is a significant way to improve their properties which would be impossible to gain by using only one reinforcement.[26] There are some studies on the mechanical behavior of the GNPs-reinforced basalt fibers/epoxy composites, such as their tensile, flexural, and high velocity impact properties.[27,28] However, to the best of our knowledge, the wear and hardness properties of these composites have not been investigated yet. Therefore, in the present study, with the aim of improving the wear properties, the effect of adding surface-modified GNPs on the sliding wear properties and microhardness of basalt fibers/epoxy composites was investigated. Moreover, attempts were made to elucidate on the mechanisms influencing the wear behavior in the nanocomposites.

EXPERIMENTAL

Materials

The epoxy matrix was KER-828 along with a polyamine hardener (HA-11) from Mokarrar Engineering Materials Co., Korea, and the weight ratio of 10:1. The woven basalt fibers were BAS 350.1270.A, Basaltex, Belgium. The GNPs were provided from the Armina Company. The silane-coupling agent, 3-amino-propyltrimethoxysilane, Merck Chemical Co., Germany, was used for the surface modification of GNPs. The properties of materials are given in Table I.

Table I. Some Properties of the Materials Used in this Study

Material	Property (unit)	Magnitude
KER 828 epoxy	Density (g/cm^3)	1.16
	Dynamic viscosity, ambient temperature (Pa s)	12–14
	Boiling point (°C)	200
	Flashpoint (°C)	200
Basalt fabrics	Wave type	Atlas
	Thickness (mm)	0.19
	Fiber diameter (μm)	12
	Areal density (g/m^2)	350
	density (g/cm^3)	2.65
	Yarn density (ends/cm)	
	Warp	15.0
	Weft	7.5
GNPs	Diameter (μm)	2–18
	Morphology	Platelet
	Color	Gray
	Purity (%)	95

Surface Modification of GNPs

For surface modification, 2.5 g of GNPs were dispersed in a water–ethanol solution (95 mL of ethanol and 5 mL of water. Using hydrochloric acid (37%), the pH of the system was adjusted in the range 2–4. Then, the silane agent 4-aminopropyltrimethoxysilane, with a weight ratio equal to that of GNPs, was added to the solution and heated to 80 °C for 8 h. The solution was then centrifuged (model RS T16) at 4000 rpm for separating the nanoparticles. Finally, the GNPs were thoroughly washed with ethanol to remove the non-functional silane compounds and dried completely in an oven.[13]

Fabrication of Nanocomposite Samples

To fabricate nanocomposite samples, different weight percentages (0, 0.1, 0.2, 0.3, 0.4, and 0.5) of the surface-modified GNPs were added to the epoxy resin and mechanically mixed at 2000 rpm for 20 min. For the proper distribution of the GNPs and preventing their agglomeration, the mixture was ultrasonicated (Fapan-400R) at a frequency of 24 Hz and a power of 120 W for 1 h.

Hybrid nanocomposites with 12 layers of basalt fibers and thickness of 4.09 mm were fabricated using the hand lay-up method. The weight ratio of basalt fibers to resin was 2:3, and the weight ratio of resin to hardener was 10:1. Finally, the samples were cured at room temperature for 1 day and post-cured at 80 °C for 120 min while subjected to 2 N/cm^2 mechanical pressure. The density of the fabricated samples was 2.76 g/cm^3.

Tests

The surface-modified GNPs were subjected to Fourier transform infrared (FTIR, Jasco 460 plus, Germany) spectroscopy in the 400–4000 cm^{-1} wavenumber range and 4 cm^{-1} sensitivity.

For friction evaluation, the pin-on-disk test was used on the nanocomposite samples (3 × 3 cm^2) according to the ASTMG-99 standard, and an average of five test results was reported. The pin was made of steel 52100 with the hardness of 800 Vickers. The pin was mounted on the lever, designed as a frictionless load transducer, and a normal load was applied during testing. For each load of 20 or 40 N, the pin rotated with the speed of 0.5 m/s and traversed a wear distance of 1000 m (Figure 1), and the path

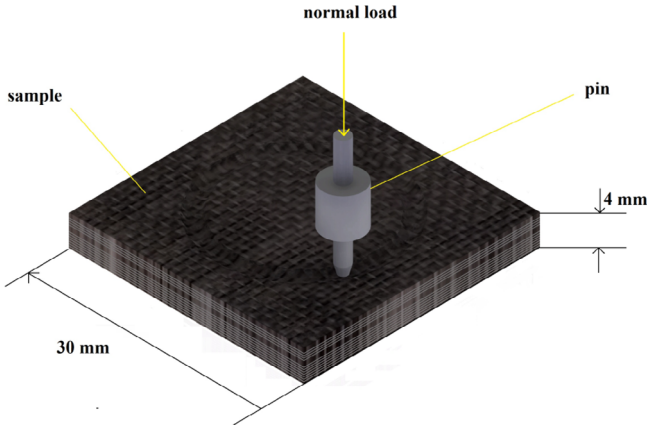

Figure 1. Schematic of a nanocomposite in pin-on-disk wear test. [Color figure can be viewed at wileyonlinelibrary.com]

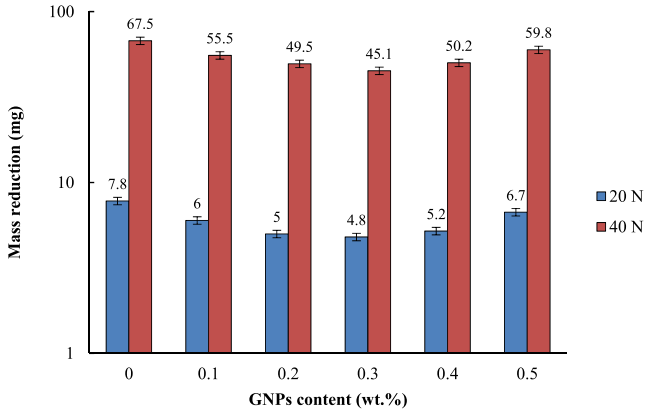

Figure 3. Mass reduction of composites versus wt % GNPs under loads of 20 and 40 N. [Color figure can be viewed at wileyonlinelibrary.com]

radius of the pin to disk was 1 cm. The Vickers microhardness of samples at five different indentation points was evaluated using a microhardness device (Buehler MHT-1B, UK).

Microscopic Analysis

To study how the GNPs influenced the wear properties of the nanocomposites, field emission scanning electron microscopy (FESEM, MIRA 3-XMU, Czech Republic) and scanning electron microscopy (SEM, VEGA\\TESCAN-XMU, Germany) were used.

RESULTS AND DISCUSSION

FTIR Spectroscopy

Figure 2 shows the FTIR spectra for both surface-modified and pristine GNPs powder. For the modified GNPs [Figure 2(a)], the broad absorption peak generated in the wave number of 1125 cm^{-1} represented the stretching vibration of C—O. In addition, the peak at 644 cm^{-1} implied the formation of C—H bond on the GNPs. The mentioned peaks were not observed in the FTIR spectra of the pristine GNPs [Figure 2(b)].

In Figure 2(a), the sharp peak at the wave number of 1462 cm^{-1} was for the formation of CH_2 and CH_3, and the peak at 1650 cm^{-1} represents the bending vibration of H—O—H.[29] Because the pristine GNPs lacked the mentioned bonds, it could be concluded that the surface modification of GNPs occurred appropriately.[12,15]

Wear Test

The mass reductions, that is, the mass loss of each nanocomposite after each wear test, are shown in Figure 3 for the 20 and 40 N loads. The results indicated that there was an optimal GNPs amount in each of the two loads) pin wear was negligible). The lowest mass

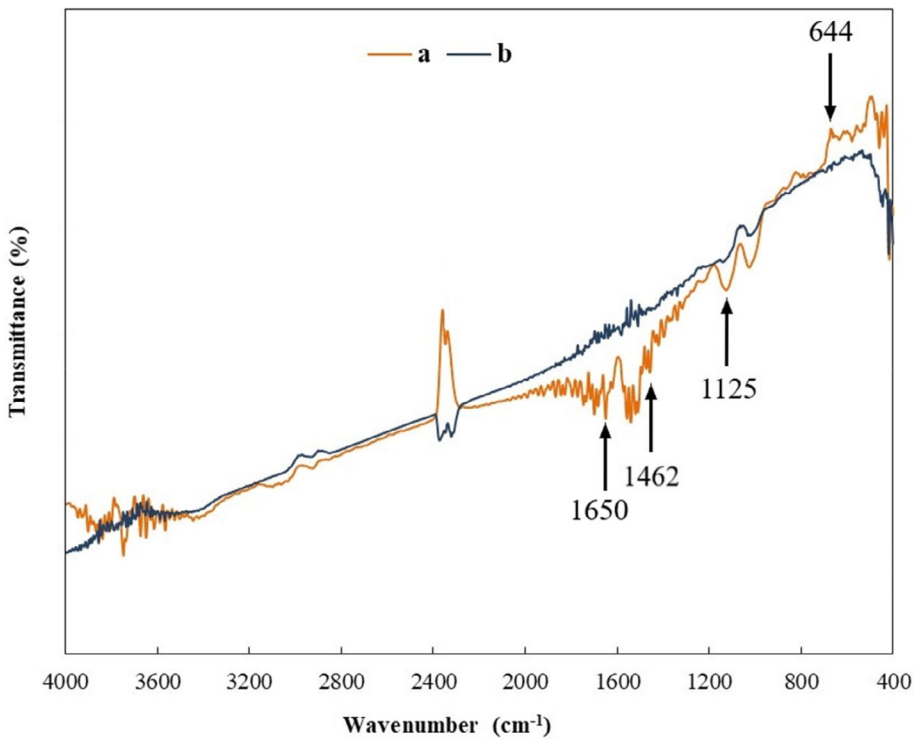

Figure 2. FTIR spectra of (a) modified GNPs, (b) pristine GNPs. [Color figure can be viewed at wileyonlinelibrary.com]

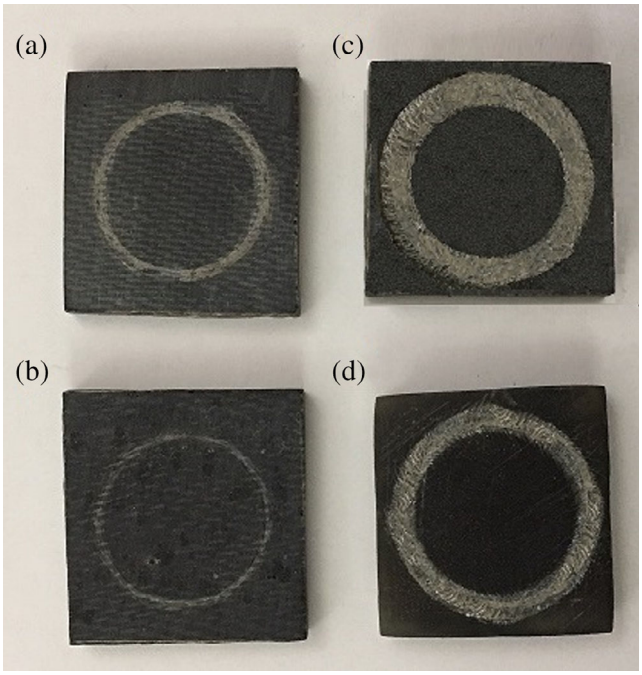

Figure 4. Pictures of the samples after wear test (a) 0.0 wt %, (b) 0.3 wt % GNPs under load of 20 N, and (c) 0.0, (d) 0.3 wt % GNPs under load of 40 N. [Color figure can be viewed at wileyonlinelibrary.com]

reduction was for the sample containing 0.3 wt % GNPs for both load levels; 38 and 33% in the 20 and 40 N loads, respectively. The effect of GNPs was not as significant in the samples containing less than 0.3 wt % GNPs as shown by their higher mass reduction. However, in the samples containing more than 0.3 wt % of GNPs, the mass reduction was higher because of the agglomeration of GNPs.

Figure 4 shows the pictures of the composites after wear test under the load of 20 and 40 N. As shown in Figure 4, the samples containing 0.3 wt % GNPs had lower mass reductions.

Figure 5 shows wear rate values for the composites containing different wt % GNPs under two load levels of 20 and 40 N. The wear rate was calculated by eq. (1):

$$W = \frac{\Delta m}{\rho F L} \quad (1)$$

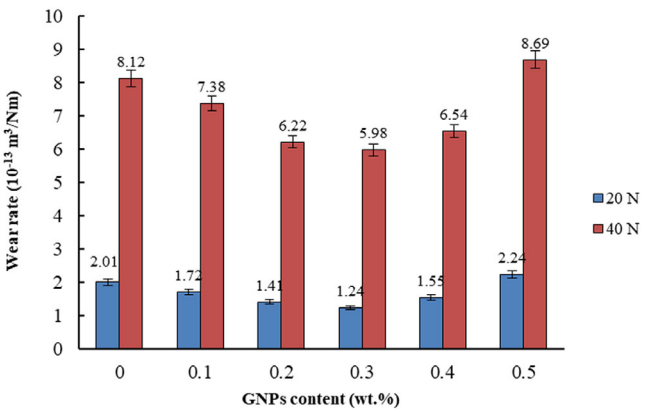

Figure 5. Wear rate of nanocomposites with different wt % GNPs under two load levels of 20 and 40 N. [Color figure can be viewed at wileyonlinelibrary.com]

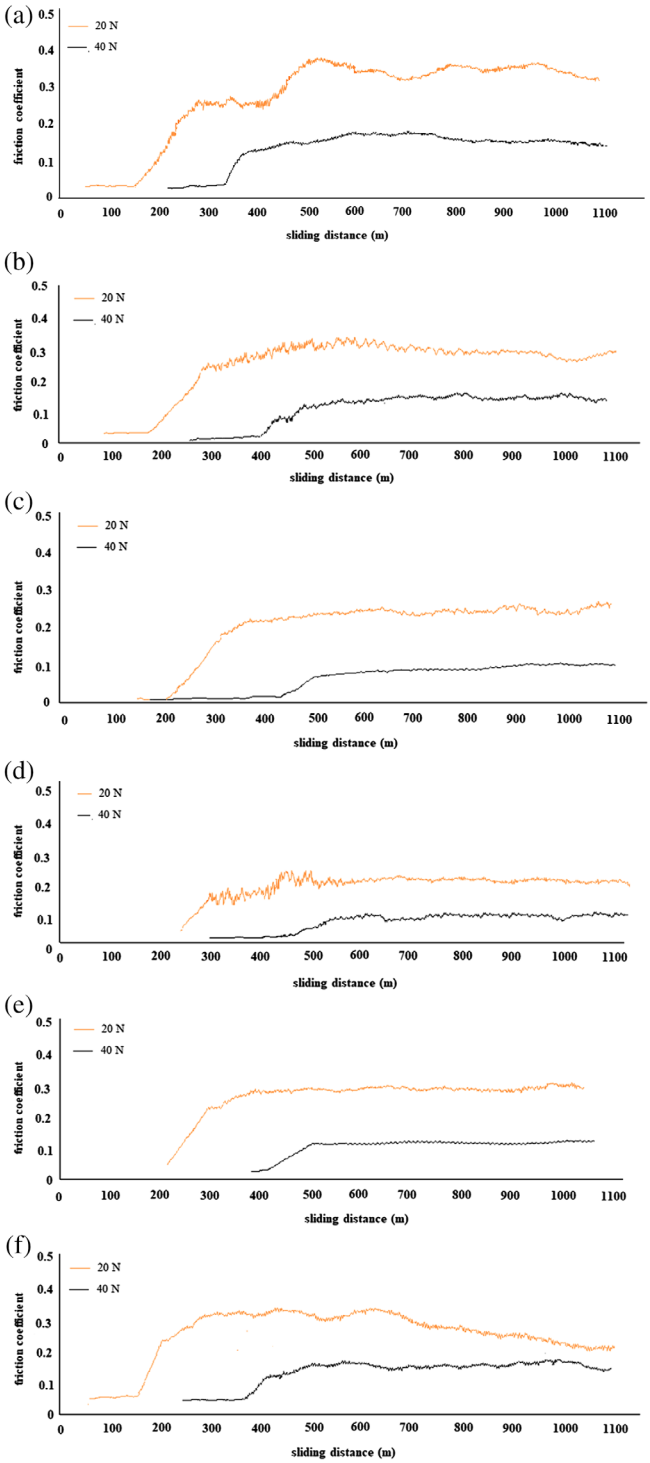

Figure 6. Friction coefficient in terms of sliding distance for nanocomposites under loads of 20 and 40 N (a) 0.0 wt %, (b) 0.1 wt %, (c) 0.2 wt %, (d) 0.3 wt %, (e) 0.4 wt %, and (f) 0.5 wt % GNPs. [Color figure can be viewed at wileyonlinelibrary.com]

where W is the wear rate, Δm is the mass reduction, ρ is the density of composites, F and L are the applied load and sliding distance, respectively.[30,31]

The overall behavior is U-shaped; the minimum belonged to the 0.3 wt % GNPs nanocomposite. Indeed, the 0.3 wt % GNPs

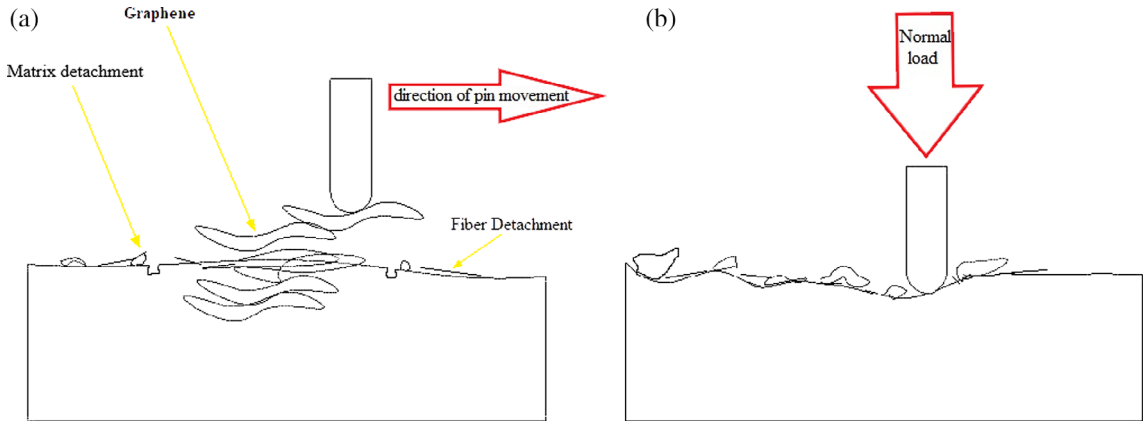

Figure 7. Schematic representation of the effective mechanism on wear behavior of basalt fibers reinforced epoxy composites (a) containing GNPs, (b) without GNPs. [Color figure can be viewed at wileyonlinelibrary.com]

nanocomposite showed lower wear rates by 45 and 40% under 20 and 40 N load levels, respectively, as compared to the composites without graphene. In the nanocomposites containing more than 0.3 wt % of GNPs, the generated transfer/lubricating films became thicker and thicker, tending to separate from the interface, thereby increasing the wear rate. Moreover, the incorporation of GNPs made the nanocomposites surface topography smoother.[32] It is known that the reduction of surface roughness leads to decrease in mechanical interlocking between the two surfaces. It is also known that the incorporation of GNPs increases the elastic modulus and stiffness of the nanocomposites leading to reduced friction by decreasing their contact with the pin.[33] Reduction of friction improved the wear attributes and thus decreased wear rate of the nanocomposites.

However, the temperature at contact surfaces increases with pin movement. This temperature rise leads to an increase in the wear rate.[30] However due to the high thermal conductivity of the GNPs, the created heat is distribute by graphene. For this reason, the composite samples containing graphene are relatively insensitive to the temperature rise in wear test.

Figure 6 shows the friction coefficient in terms of the sliding distance in pin-on-disk tests for nanocomposites of different wt % GNPs under two levels of loads 20 and 40 N.

The friction coefficient in all nanocomposites and in both load levels initially increased sharply and then plateaued. The difference among these diagrams was in the initial increase. Considering each case separately, it could be seen that in the composite without GNPs, the initial increase in the friction coefficient was sharper.[4] This indicated that the composite traversed a longer distance under hard frictional conditions and thus both mass reduction and wear rate were high. As a result, the composite without GNPs did not have a good wear behavior, as compared to the nanocomposites under both load levels. As shown in Figure 6(d), the nanocomposite containing 0.3 wt % GNPs had the lowest maximum friction coefficient under both load levels. Also, this sample reached its maximum friction coefficient at a lower rate as compared to all other samples. In other words, this nanocomposite reached the maximum friction coefficient upon traveling the longest distance. This is attributed to the presence of GNPs and thus the formation of a stable transfer/lubricating film.[24]

As known, the multi-layer GNPs possessing weak van der Waals bonding easily slide under the shear load and provide a self-lubrication property unto the nanocomposite..[19] The self-lubrication mechanism of GNPs on wear behavior of basalt fibers/epoxy composites is schematically illustrated in Figure 7. This behavior led to the improvement in the wear property of the nanocomposites containing GNPs.

For contents beyond 0.3 wt %, agglomeration of the GNPs took place and thus the distance traversed to reach the maximum friction coefficient was lower. These nanocomposites traversed the most of the sliding distance while experiencing the maximum friction coefficient. In other words, in these nanocomposites, the friction coefficient increased due to the adverse effect of GNPs' agglomeration. As for the two different loads, the friction coefficient in all nanocomposites decreased at the higher load. Furthermore, the high frictional load caused continuous separation and shearing off at the composite/disk interface, preventing the formation of a stable transfer/lubricating film; that is why the coefficient of friction remained high.[34]

The average friction coefficient for the nanocomposites containing different wt % GNPs at two different loads is shown in

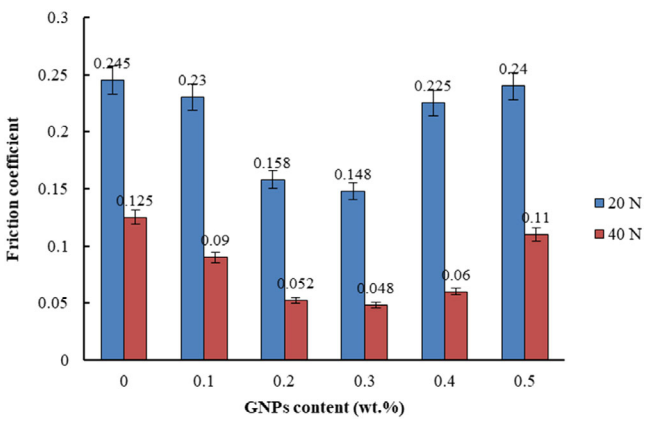

Figure 8. Friction coefficient for composites with different wt % GNPs under two load levels of 20 and 40 N. [Color figure can be viewed at wileyonlinelibrary.com]

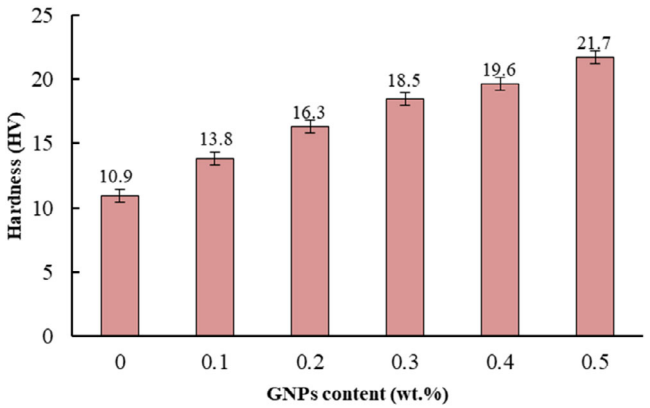

Figure 9. Microhardness test results for the nanocomposites containing different wt % GNPs. [Color figure can be viewed at wileyonlinelibrary.com]

Figure 8. The behavior is U-shaped; decreased to a minimum and then increased with wt % GNPs. The average friction coefficient for the 0.3 wt % nanocomposite decreased by 61.2 and 39.5%, respectively, for the 20 and 40 N loads.

The friction behavior aforementioned regarding the effect of GNPs and load could be explained by eqs. (2)–(4)[35–37]:

$$\mu = \frac{F}{W} \tag{2}$$

$$F = \tau A \tag{3}$$

$$\mu = \frac{\tau A}{W} \tag{4}$$

where μ is the friction coefficient, F is the friction force, W is the normal load, τ is the shear strength, and A is the total area of contact.

Equation (4) can be derived from eqs. (2) and (3). Indeed with increasing the normal load, the contact temperature between the composite and pin will be increased due to the frictional heat, which results in two contrary effects on the friction coefficient. First, the increase in temperature leads to a decrease in the shear strength of the basalt fiber reinforced epoxy and consequently the friction coefficient. Second, higher temperature leads to reduce the elastic modulus of the material and increase in the contact area. According to eq. (4), the friction coefficient would increase by this event. Hence, the final friction coefficient would be determined by two parameters. In the case of our material, as can be observed in Figure 8, the friction coefficient is decreased at a higher normal load. It can be concluded that the decrease in shear strength is dominant and an increase in the normal load (W) results in a reduction of the friction coefficient (μ).[31] Moreover, in constant normal loads, easy sliding within the GNPs caused a reduction in the shear strength leading to a lower friction coefficient. This corresponds to the experimental results obtained in this study.

Microhardness Test

The surface hardness is one of the most important factors that control the wear resistance of the materials. Therefore, the microhardness of the nanocomposites was measured.

The microhardness test results for the nanocomposite samples containing different wt % GNPs are shown in Figure 9. The overall trend is upward and almost linear. The maximum hardness of 21.7 HV was achieved for the 0.5 wt % GNPs nanocomposite, which showed 99% increase in comparison to the composite without GNPs. The microhardness enhancement was mainly due to the internal and 3D stresses the presence of GNPs generated.[26]

Microscopic Analysis

The FESEM and SEM micrographs from the surface of the composite samples verified the results of the wear test (Figures 10–13). The presence of GNPs enhanced the adhesion between the fibers and the matrix.[38,39] Figure 10 shows the FESEM images of the wear surfaces for composites containing 0.0 wt %, 0.3 wt %, and 0.5 wt % GNPs under the load of 20 N. As shown in Figure 10(a), in the sample without GNPs, because of the low adhesion between

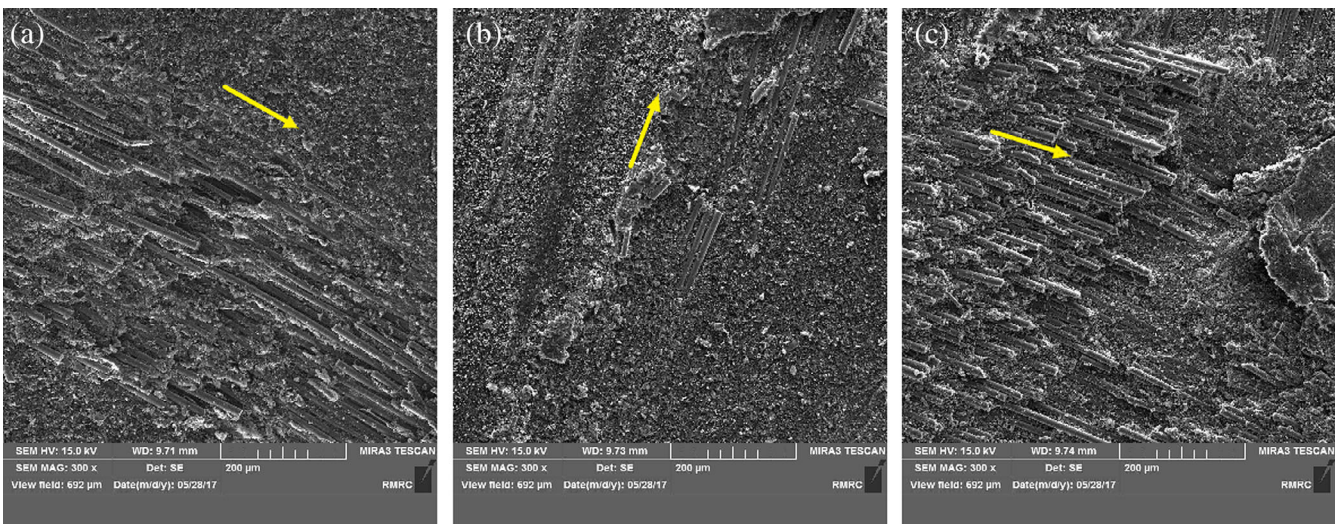

Figure 10. FESEM images of the composite wear surfaces with (a) 0.0 wt %, (b) 0.3 wt %, and (c) 0.5 wt % GNPs under load of 20 N. [Color figure can be viewed at wileyonlinelibrary.com]

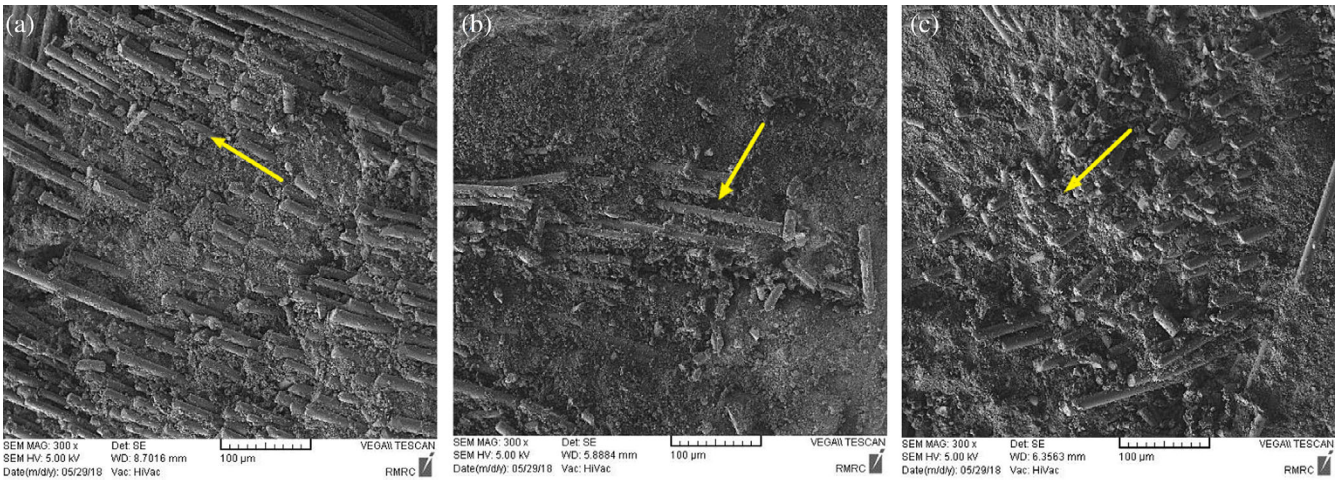

Figure 11. SEM images of the composite wear surfaces containing (a) 0.0 wt %, (b) 0.3 wt %, and (c) 0.5 wt % GNPs under load of 40 N. [Color figure can be viewed at wileyonlinelibrary.com]

the fibers and the resin, the resin was removed from the surface of the fibers by wear, and the resin-free fibers could be observed on the surface of the sample. The presence of these fibers at the surface helped in increasing the wear rate and thus reduction of the wear resistance.

As can be observed in Figure 10(b), at fewer areas, the resin has been removed from the surface of the fibers, indicating that the fibers, contrary to the sample without GNPs, were not affected as much by the pin movement during friction and thus the wear of fibers in this sample was less as compared to the sample without GNPs. Figure 10(b) also shows the enhanced adhesion between fibers and resin due to the presence of GNPs. Moreover, the weak van der Waals bonds between the lamellae of GNPs (low shear resistance) facilitated the reduction of damage and friction under the shear stress of the abrasive agent.[35]

The wear surface of the 0.5 wt % GNPs nanocomposite is shown in Figure 10(c). As demonstrated earlier, beyond 0.3 wt %, the GNPs agglomerated within the resin matrix, causing undesirable wear; they did not participate in the self-lubrication mechanism during wear. This is despite the fact that their presence up to 0.5 wt % helped in enhancing the microhardness. The microhardness enhancement was mainly due to the internal and 3D stresses the presence of GNPs generated.

Figure 11 shows the SEM images of the wear surfaces for composites containing 0.0 wt % and 0.3 wt % GNPs under the load of 40 N. As compared to those tested at 20 N, the surfaces of the samples received more damage. The detachment of resin from fibers led to the exposure of fibers to the sliding wear contact and thus breakage of the fibers. These general observations from Figures 10 and 11 verified the results of Figure 3.

The presence of GNPs on the wear surface for the nanocomposite containing 0.3 wt % GNPs is shown in Figure 12. The GNPs on the wear surface acted as a lubricating agent and reduced the coefficient of friction.

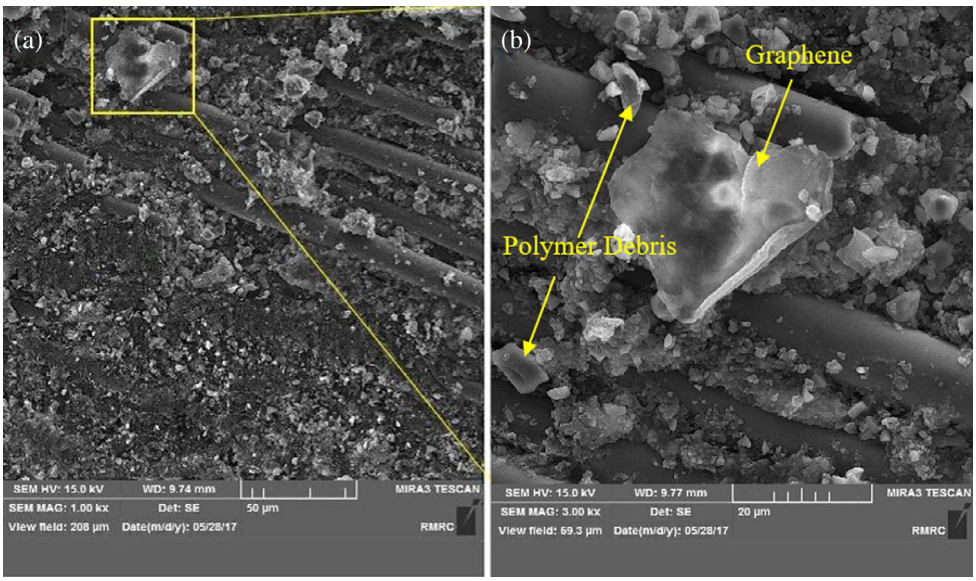

Figure 12. GNPs on the wear surface of the 0.3 wt % GNPs nanocomposite. [Color figure can be viewed at wileyonlinelibrary.com]

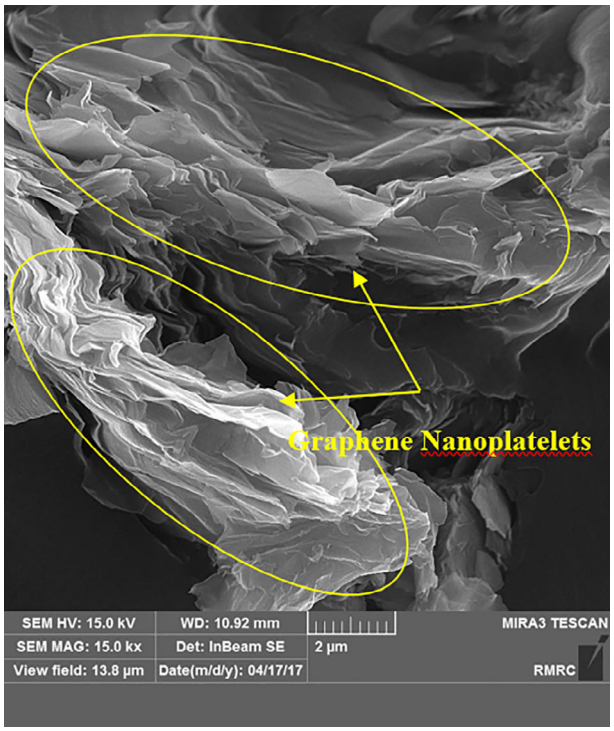

Figure 13. FESEM image of agglomerated GNPs on the wear surface of a nanocomposite containing 0.5 wt % GNPs. [Color figure can be viewed at wileyonlinelibrary.com]

The FSEM and SEM images of the worn surfaces of the composites without GNPs show signs of fatigue wear because of deep grooves and debris. In fact, the mechanisms of wear in polymers are a combination of fatigue and abrasion. Fatigue is usually related to low wear resistance and, consequently, high amounts of debris. The amounts of debris on the worn surface of composites without GNPs clearly prove that fatigue-delamination occurred with repeated loading during sliding [Figures 10(a) and 11(a)]. However, this mechanism is negligible for the 0.3 wt % GNPs nanocomposite, resulting in higher wear resistance [Figures 10(b) and 11(b)], In other words, the wear mechanism changed from fatigue (no GNPs) to abrasive (0.3 wt % GNPs), thus decreased the mass reduction.[40,41]

Figure 13 shows the agglomeration of GNPs on the wear surface of the 0.5 wt % GNPs nanocomposite. This agglomeration caused undesirable wear and reduced the wear resistance in the nanocomposite.

CONCLUSIONS

The effects of adding surface-modified GNPs (0.1, 0.2, 0.3, 0.4, and 0.5 wt %) on the wear properties of basalt fibers-reinforced epoxy composites under the load levels of 20 and 40 N were investigated. The following conclusions were drawn:

- The addition of surface-modified GNPs improved the microhardness and wear properties of the composites considerably.
- The best microhardness result was achieved with 0.5 wt % GNPs; nearly 100% in comparison to the sample without GNPs. The presence of GNPs generated internal and 3D stresses that caused stronger composites.
- The best wear properties were achieved with 0.3 wt % GNPs for both loads of 20 and 40 N; beyond 0.3 wt %, the GNPs agglomerated and wear properties deteriorated.
- GNPs' self-lubrication property improved the wear properties in the best nanocomposite (0.3 wt % GNPs) by generating a thin and stable transfer/lubricating film. These results corresponded to the theoretical prediction.

REFERENCES

1. Shen, X. J.; Pei, X. Q.; Fu, S.-Y.; Friedrich, K. *Polymer*. **2013**, *54*, 1234.
2. Yasmin, A.; Daniel, I. M. *Polymer*. **2004**, *45*, 8211.
3. Friedrich, K.; Lu, Z.; Häger, A. *Theor. Appl. Fract. Mech.* **1993**, *19*, 1.
4. Saurín, N.; Sanes, J.; Bermúdez, M. *Tribol. Lett.* **2014**, *56*, 133.
5. Mohan, N.; Mahesha, C.; Mathivanan, N. R.; Shivamurthy, B. *Procedia Eng.* **2013**, *64*, 1166.
6. Golchin, A.; Wikner, A.; Emami, N. *Tribol. Int.* **2016**, *95*, 156.
7. Dasari, A.; Yu, Z.-Z.; Mai, Y.-W.; Hu, G.-H.; Varlet, J. *Compos. Sci. Technol.* **2005**, *65*, 2314.
8. Shen, X.-J.; Liu, Y.; Xiao, H.-M.; Feng, Q.-P.; Yu, Z.-Z.; Fu, S.-Y. *Compos. Sci. Technol.* **2012**, *72*, 1581.
9. Rathore, D. K.; Prusty, R. K.; Kumar, D. S.; Ray, B. C. *Composites Part A*. **2016**, *84*, 364.
10. Hu, K.; Kulkarni, D. D.; Choi, I.; Tsukruk, V. V. *Prog. Polym. Sci.* **2014**, *39*, 1934.
11. Bafana, A. P.; Yan, X.; Wei, X.; Patel, M.; Guo, Z.; Wei, S.; Wujcik, E. K. *Composites Part B*. **2017**, *109*, 101.
12. Cui, Y.; Kundalwal, S.; Kumar, S. *Carbon*. **2016**, *98*, 313.
13. Bahari-Sambran, F.; Eslami-Farsani, R.; Arbab Chirani, S. *J. Sand. Struct.* **2018**, *21*, 1.
14. Zhang, W.; Schröder, C.; Schlüter, B.; Knoch, M.; Dusza, J.; Sedlák, R.; Mülhaupt, R.; Kailer, A. *Tribol. Lett.* **2018**, *66*, 121.
15. Liu, M.; Duan, Y.; Wang, Y.; Zhao, Y. *Mater. Des.* **2014**, *53*, 466.
16. Soldano, C.; Mahmood, A.; Dujardin, E. *Carbon*. **2010**, *48*, 2127.
17. Schedin, F.; Geim, A.; Morozov, S.; Hill, E.; Blake, P.; Katsnelson, M.; Novoselov, K. S. *Nat. Mater.* **2007**, *6*, 652.
18. Pan, B.; Zhang, S.; Li, W.; Zhao, J.; Liu, J.; Zhang, Y.; Zhang, Y. *Wear*. **2012**, *294*, 395.
19. Yang, J.; Xia, Y.; Song, H.; Chen, B.; Zhang, Z. *Tribol. Int.* **2017**, *105*, 118.
20. Zhang, H.-B.; Zheng, W.-G.; Yan, Q.; Yang, Y.; Wang, J.-W.; Lu, Z.-H.; Ji, G. Y.; Yu, Z. Z. *Polymer*. **2010**, *51*, 1191.
21. Kuilla, T.; Bhadra, S.; Yao, D.; Kim, N. H.; Bose, S.; Lee, J. H. *Prog. Polym. Sci.* **2010**, *35*, 1350.
22. Georgakilas, V., Otyepka, M., Bourlinos, A.B., Chandra, V., Kim, N., Kemp, K.C., Hobza,P. Zboril,R. Kim, K. S. *Chem. Rev.* **2012**, *112*,6156–6214, .
23. Wu, F.; Zhao, W.; Chen, H.; Zeng, Z.; Wu, X.; Xue, Q. *Surf. Interface Anal.* **2017**, *49*, 85.

24. Ren, G.; Zhang, Z.; Zhu, X.; Ge, B.; Guo, F.; Men, X.; Liu, W. *Composites Part A*. **2013**, *49*, 157.
25. Bahadur, S.; Sunkara, C. *Wear*. **2005**, *258*, 1411.
26. Chang, L.; Friedrich, K. *Tribol. Int.* **2010**, *43*, 2355.
27. Bulut, M. *Composites Part B*. **2017**, *122*, 71.
28. Kazemi-Khasragh, E.; Bahari-Sambran, F.; Siadati, M. H.; Eslami-Farsani, R. *Fibers Polym.* **2018**, *19*, 2388.
29. Romanzini, D.; Piroli, V.; Frache, A.; Zattera, A. J.; Amico, S. C. *Appl. Clay Sci.* **2015**, *114*, 550.
30. Davim, J. P.; Cardoso, R. *Wear*. **2009**, *266*, 795.
31. Meng, H.; Sui, G.; Xie, G.; Yang, R. *Compos. Sci. Technol.* **2009**, *69*, 606.
32. Khun, N. W.; Zhang, H.; Lim, L. H.; Yang, J. *Appl. Sci. Technol*. **2015**, *8*, 101.
33. Khun, N. W.; Zhang, H.; Yang, J.; Liu, E. *Wear*. **2012**, *296*, 575.
34. Liu, L.; Yan, F.; Gai, F.; Xiao, L.; Shang, L.; Li, M.; Ao, Y. *RSC Adv.* **2017**, *7*, 33450.
35. Yang, M.; Zhang, Z.; Zhu, X.; Men, X.; Ren, G. *Friction*. **2015**, *3*, 72.
36. Stuart, B. *Polym. Test.* **1997**, *16*, 49.
37. Maegawa, S.; Itoigawa, F.; Nakamura, T. *Tribol. Int.* **2015**, *92*, 335.
38. Galpaya, D.; Wang, M.; Liu, M.; Motta, N.; Waclawik, E. R.; Yan, C. *Graphene*. **2012**, *1*, 30.
39. Qin, W.; Vautard, F.; Drzal, L. T.; Yu, J. *Composites Part B*. **2015**, *69*, 335.
40. Baptista, R.; Mendão, A.; Rodrigues, F.; Figueiredo-Pina, C.; Guedes, M.; Marat-Mendes, R. *Theor. Appl. Fract. Mech.* **2016**, *85*, 113.
41. Hutchings, I. Tribology: Friction and Wear of Engeeniring Materials; Heineman: London, **1992**.